

## STIFFENING THE CORNEA: THE THERAPEUTIC POTENTIAL OF GLYCATION

5.1 Introduction .....	109
5.2 Materials and Methods .....	111
5.3 Mechanical Properties of Glycated Corneas .....	116
5.4 Resistance to Proteolytic Degradation.....	118
5.5 Quantification of Specific AGEs .....	120
5.6 Solution and Solid-State NMR of Glycated Corneas.....	123
5.7 Fluorescence – Noninvasive Indicator of Glycation .....	126
Bibliography .....	130

**5.1 Introduction**

Whereas the goal of our vitreous efforts was liquefaction, our therapeutic objective in the cornea is fortification. The primary purpose of fortification is the treatment of keratoconus, a disease in which the cornea softens and subsequently bows under the influence of intraocular pressure (as explained in Chapter 1). Here, we present the biochemical modifications and concomitant mechanical reinforcement that result from treating corneal tissue with glyceraldehyde (GA), a reducing sugar known to crosslink proteins through a complex series of reactions known as the Maillard reaction.<sup>1</sup>

The Maillard reaction, initially characterized as the browning of proteins treated with reducing sugars, results in the non-enzymatic glycosylation (glycation) of amino acids with primary amine groups, particularly lysine and arginine. Over the past two decades, some intermediates and advanced glycation end products (AGEs) of these reactions have been

characterized,<sup>2-14</sup> including cross-linking structures<sup>2-6, 13, 14</sup> that may be responsible for the increased tissue stiffness and decreased protein solubility also characteristic of glycation.<sup>15-18</sup>

While glycation has primarily been explored because of its apparent connection with health problems<sup>19-23</sup> associated with diabetes<sup>16, 24</sup> and aging,<sup>25, 26</sup> if properly harnessed this nonenzymatic crosslinking method has potential therapeutic and tissue engineering applications.<sup>27-29</sup> By imparting strength to weakened connective tissue such as diseased corneas, glycation may provide an alternative to tissue transplants in diseases such as keratoconus. Glycation may also be a helpful tool for adding mechanical strength to protein-based and polyamide synthetic tissues.

Understanding glycation-induced stiffening and quantitative indicators thereof is necessary for understanding the pathology of natural glycation and for utilizing its positive potential. However, a quantitative correlation between the formation of specific AGEs and physiologically-significant tissue stiffening has not previously been established. Furthermore, previous studies on the biomechanical influences of glycation have employed methods based upon tissue failure, which do not demonstrate whether the stiffening effects of glycation are significant under physiological stresses.<sup>26</sup>

In the present work, rotational rheometry has been used in combination with analytical biochemistry to explore the therapeutic potential of GA for treating keratoconus. GA is an appealing glycating agent for tissue engineering because of its relatively high reactivity and low toxicity.<sup>30</sup> Small amplitude oscillatory shear stresses have been applied to probe the

mechanical response of porcine corneas to physiologically relevant stresses, which do not destroy the nanostructure of the tissue. We have correlated the rise in shear modulus of porcine corneas with the levels of one non-cross-linking and two cross-linking AGEs (Figure 1).<sup>9, 14</sup> We have also examined the stabilizing effect of glycation against enzymatic degradation. Finally, solid-state NMR of the treated corneas and solution NMR of their lysates are compared to investigate the merits of enzymatic digestion versus acid hydrolysis for AGE isolation.

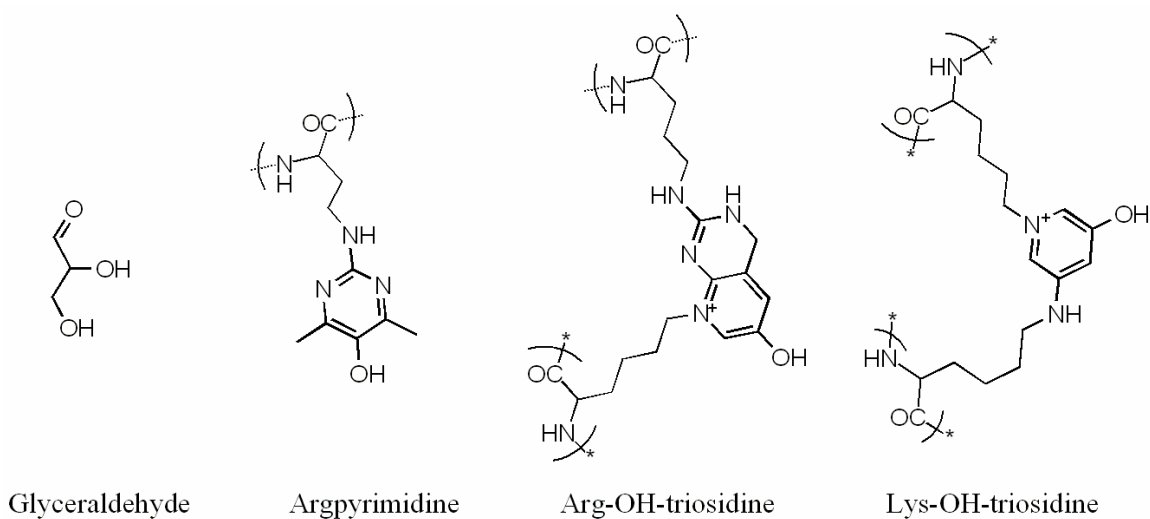


Figure 1. The structure of glycerinaldehyde and three of its AGEs

## 5.2 Materials and Methods

*Materials* – Fresh porcine eyes (< 36 hours *post mortem*, stored at 5° C in physiological saline prior to arrival) were acquired through Sierra for Medical Science (Santa Fe Springs, CA). All pigs were 3 – 6 month old Chester Whites, weighing 50 – 100 kg and in good

health at the time of slaughter. 99% [U-<sup>13</sup>C]glyceraldehyde was obtained from Cambridge Isotope Laboratories Inc. (Andover, MA). Argpyrimidine, Arg-hydroxy-triosidine, and Lys-hydroxy-triosidine were synthesized and purified as described previously.<sup>14</sup> All other enzymes and reagents were purchased from Sigma Chemical Co. (St. Louis, MO).

*Cornea sample preparation* – Corneas were excised from fresh porcine eyes. An 8.0 mm circular section was cut from the center of each using a trephine from Jedmed Instrument Co. (St. Louis, MO), washed in metal-free 200 mM phosphate buffer solution pH 7.4 (PBS), and weighed (typical wet weight = 60 mg). The epithelium of each sample was removed and corneas were either characterized directly to obtain “native” rheological and biochemical properties or treated according to the following regimen: 30 µl of either PBS, 1% (weight of dry GA / weight of solution) GA in PBS (0.3 mg GA), or 2% GA in PBS (0.6 mg GA) was applied topically. In all cases, 1 µl each of toluene and chloroform were added per ml treatment solution to prevent bacterial growth. Corneas were incubated in sealed tubes at 37° C for 2 or 6 days and rheological and/or biochemical measurements were made immediately thereafter; at least 6 repetitions of each treatment were made.

*Rheology* – Oscillatory shear modulus measurements under controlled stress were made using AR2000 and SR5000 stress-controlled rheometers from TA Instruments (New Castle, DE). The anterior and posterior surfaces of corneas were gently dried by contact with an absorbent pad (< 3% weight change as noted in Chapter 2) and immediately loaded on 8 mm parallel disc fixtures at 25° C. The dynamic moduli were found to be highly sensitive to hydration levels; therefore, a solvent trap and well were used to prevent

evaporation and hydrate the air within the sample chamber. To obtain mechanical properties representative of physiologically relevant stresses, measurements were performed using small oscillatory shear stresses ( $\sigma = 5$  Pa). After the rheological data were collected, the corneas were used either for solid-state  $^{13}\text{C}$ -NMR, digested for HPLC, protein content analyses, fluorescence spectroscopy, and solution state  $^{13}\text{C}$ -NMR, or acid hydrolyzed for HPLC.

*Solid-state NMR* – Digestion was not necessary to prepare samples for solid-state NMR. To remove  $^{13}\text{C}$ -bearing compounds not covalently bound, corneas were washed in 200 mM phosphate buffer solution pH 7.4 and lyophilized for analysis. In each experiment, 6 treated corneas were packed into a 7 mm  $\text{ZrO}_2$  rotor and spun (rate = 4.0 kHz) at the magic angle.  $^{13}\text{C}$  Solid-state NMR direct polarization (Bloch decay) spectra of lyophilized cornea samples were obtained using a Bruker 200 DSX spectrometer (Bruker BioSpin Corp., MA). The probe was doubly tuned for  $^1\text{H}$  and  $^{13}\text{C}$  observation at frequencies of 200.1 MHz and 50.3 MHz, respectively. 8,000 scans were acquired in each measurement with a 20 second delay time between scans. All solid-state NMR experiments were conducted by Dr. Sonjong Hwang (Caltech SSNMR facility manager) and Dr. Giyoong Tae (former Kornfield group member).

*Enzymatic Digestion* – The greater the extent of glycation, the more difficult it is to solubilize the cornea. To do so with minimal change to the chemical structures of the pendant adducts and crosslinks, an enzymatic digestion protocol was used rather than acid hydrolysis. Acid hydrolysis completely hydrolyzes peptide bonds.<sup>31</sup> However, it also destroys some amino acids (e.g. tryptophan) and AGEs. To access acid-labile AGEs, we

employ a gentle, enzymatic method for solubilizing cornea proteins via sequential incubation in collagenase, pronase E, and proteinase K. Glycated corneas were gently agitated for 24 hours at 37° C in these three complimentary proteinases in succession. 2% (weight dry enzyme / wet weight of cornea) collagenase A in 100 mM HEPES buffer solution, pH 7, and 5 mM calcium chloride was used for the first digestion. 1 µl each of toluene and chloroform were added per ml digestion solution to prevent bacterial growth as with the treatment solutions. After the 24 hour incubation period, the cornea mixture was centrifuged to pellet insoluble cornea fragments and the supernatant was collected for protein content and NMR analyses. The supernatant was replaced with a 2% pronase E solution in 100 mM HEPES buffer, pH 7.5, and 5 mM calcium chloride and again agitated for 24 hours at 37° C. After the pronase E incubation, the cornea mixture was again centrifuged to pellet residual cornea fragments, and the supernatant was collect. A third solution, containing 2% proteinase K in 100 mM Tris buffer, pH 8.0, and 5 mM calcium chloride was added for the final incubation. After 24 hours in the proteinase K solution, the supernatant was collected and the final pellet was rinsed in PBS and then dried for acid hydrolysis. The bovine serum albumin (BSA)-equivalent protein content of each lysate solution was determined by absorbance measurements at 210 nm; the respective enzyme solutions were used as blanks.

No organic buffers (e.g., HEPES or TRIS) were used in the enzymatic digests for solution-state NMR because it was found that the naturally abundant <sup>13</sup>C in the buffer mask the adduct signals. Phosphate buffer could not be used because it would chelate calcium ions needed for enzymatic activity. Solution-state NMR digestions were conducted in 0.9%

saline, pH 7.4 – 7.6. To compensate for the likely reduction in enzyme activity due to deviation from optimal pH late in the incubation periods, the concentration of CaCl<sub>2</sub> added to collagenase and proteinase K solutions was increase from 5 to 10 mM.

*Acid Hydrolysis* – Insoluble protein aggregates from the enzymatic digest were dissolved by acid hydrolysis in 0.5 ml of 6 N HCl for 16 hours at 110° C for analysis. Nine untreated corneas and two sets of six glycated corneas were also hydrolyzed under the same conditions in 2 ml of 6 N HCl. After hydrolysis, the acid was evaporated and samples were reconstituted in water. Leucine-equivalent amino acids were measured by the ninhydrin assay to determine protein content.

*Glycation Product Identification and Quantification by High Performance Liquid Chromatography (HPLC)* – A Waters HPLC system including an in-line degasser, 600 controller, 717 autosampler, 996 photodiode array detector, 474 scanning fluorescence detector (monitored at 380 nm with an excitation wavelength of 325 nm), and Millennium software (Waters corporation, MA) were used. Each sample was filtered with a Costar Spin-X 0.45 µm cellulose acetate filter (Corning Incorporated, NY) prior to injection into the HPLC system. Separations were made on a 250 x 4.6 mm Discovery C18 column, 3 µm (Supelco, PA), protected by a 20 x 4.0 mm Supelguard Discovery C18 column, 5 µm. Peak collection was performed using a FRAC-100 fraction collector (Amersham Pharmacia Biotech, Sweden). Adduct quantification was achieved by method of external standard, where chromatogram peak area by fluorescence detection was used to quantify adducts formed as described in detail by Tessier, et al.<sup>14</sup> HPLC analyses were conducted

with Dr. Tessier (former Kornfield group member) and results appeared in the aforementioned reference.

*Solution NMR* – After digestion each cornea solution was concentrated using a Speed Vac Plus SC110A (Savant Inc., NY). The concentrated fractions were pooled and dissolved in 700  $\mu$ l of 99% D<sub>2</sub>O for <sup>13</sup>C-NMR analysis. The samples were transferred to 5 mm glass NMR tubes (Kontes glass company, NJ). <sup>13</sup>C solution NMR spectra of digested cornea solutions were taken on a Varian 500 MHz spectrometer at 25° C (Varian Inc., CA). For quantitative analysis, the proton decoupling was turned off during excitation and a 20-second delay time was used. Acetonitrile was added to each NMR sample as a standard.

*Spectrometry* – Fluorescence spectra of the protein digest solutions of each cornea were recorded with a Photon Technology International spectrofluorometer (Photon Technology International, NJ). Individual adducts were prepared for fluorescence measurements by purifying, concentrating, and redissolving each in pure water as described by Tessier, et al.<sup>14</sup> UV-Visible absorbance measurements for ninhydrin protein content analyses were recorded with a Beckman DU 640 spectrophotometer (Beckman Instruments Inc., CA).

### **5.3 Mechanical Properties of Glycated Corneas**

The shear modulus of corneal tissue increased upon treatment with GA in a dose-dependent fashion (Figure 2). Relative to the mean modulus of corneal buttons incubated in phosphate buffer ( $457 \pm 142$  Pa,  $n = 7$ ), the mean modulus of corneas treated with 1% GA ( $1359 \pm 372$  Pa,  $n = 6$ ) and 2% GA ( $2862 \pm 467$  Pa,  $n = 8$ ) increased by 300% ( $P < 0.0001$ ) and

600% ( $P < 0.0001$ ), respectively, after 2 days. Rheological properties at day 6 of incubation ( $2904 \pm 349$  Pa,  $n = 5$ ) did not change significantly from day 2.

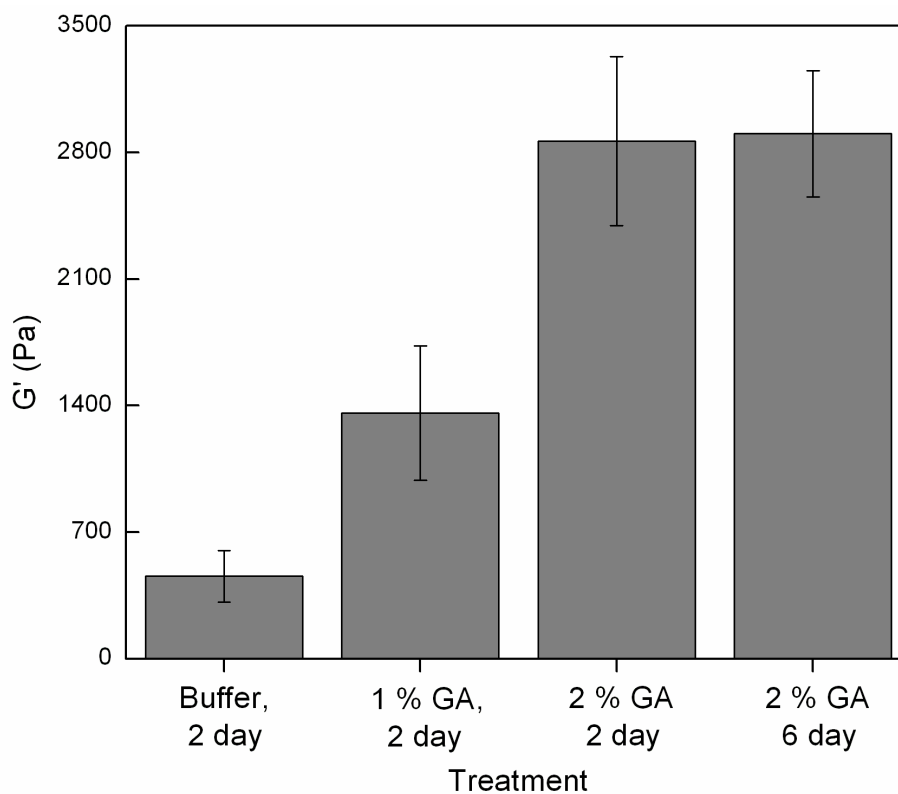


Figure 2. Modulus increases with treatment. Stiffening goes to completion within 2 days; additional incubation time yields no change.

Prior literature indicates that the level of mechanical reinforcement obtained with application of 2% GA is more than sufficient to stabilize the keratoconus cornea. Using a protein crosslinking strategy that involves topical application of riboflavin and UV irradiation, Wollensak et al. showed that stiffening keratoconus corneas by  $\sim 350\%$  was sufficient to stop coning for at least three years.<sup>32,33</sup> They also showed that porcine corneas,

which are x1.5 thicker (850  $\mu\text{m}$  vs. 550  $\mu\text{m}$ ), stiffened by only 80% when subject to the same level of treatment. Using this ratio (80% stiffening in porcine cornea is equivalent to 350% stiffening in human tissue) as a guide, we anticipate that treating human corneas with significantly less than 1% GA, which stiffened *porcine* corneas by 300%, would be sufficient to stop the progression of keratoconus.

GA treatment may offer advantages over riboflavin treatment: UV irradiation is not required, reducing the likelihood of keratocyte apoptosis<sup>34</sup> and cataracts<sup>35</sup>, and we observed that GA-treated corneas yellow much less than corneas treated with riboflavin/UV irradiation. Having demonstrated that glycation with GA can produce therapeutically significant improvement in the mechanical properties of the cornea, we proceed to analyze its biochemical impact.

#### **5.4 Resistance to Proteolytic Degradation**

The most significant biochemical benefit to treating keratoconus by glycation may be the increased resistance to enzymatic digestion. The cornea is composed of 78% water, 15% collagen type I fibrils, 5% other proteins, 0.7% keratin sulfates, 0.3% chondroitin sulfates, and 1% salts.<sup>36</sup> It has been proposed that the softening associated with keratoconus is the result of abnormally high protease activity against collagen.<sup>37-40</sup> A number of enzymes are over expressed in keratoconus corneas, including acid esterase, acid phosphatase, and matrix metalloproteinases 2 and 9.<sup>40-42</sup> Glycation decreases the susceptibility of collagenous tissues to proteolytic degradation.<sup>43</sup> Thus, in addition to its mechanical

benefits, the proposed GA treatment may also arrest the pathologic mechanism behind mechanical destabilization.

Our results confirm that glycation of the cornea with therapeutic doses of GA has a protective effect against collagenase. Corneas glycated with 2% GA are approximately 1/10 as susceptible to collagenase solubilization as buffer-treated controls, though pronase appears to work relatively efficiently even after treatment (Figure 3). Glycation reduces the total fraction of protein solubilized after exposure to all three enzymes from > 90% to ~ 50%, but by far the bulk of that reduction is in the collagenase incubation. This suggests that the unglycated collagen helices in treated corneas are preferentially solubilized, which would leave the insoluble fragments with a disproportionately high fraction of AGEs. HPLC analysis corroborates this conclusion: only trace amounts of the AGEs triosidine and argpyrimidine were detected in the soluble portion of the enzymatic lysates, whereas HPLC analysis of the precipitate (solubilized by subsequent acid hydrolysis) showed substantial amounts of these acid-stable adducts. The inability to solubilize heavily-glycated proteins using gentle methods that preserve acid-labile AGEs was the primary motivation for analyzing native samples using solid-state NMR.

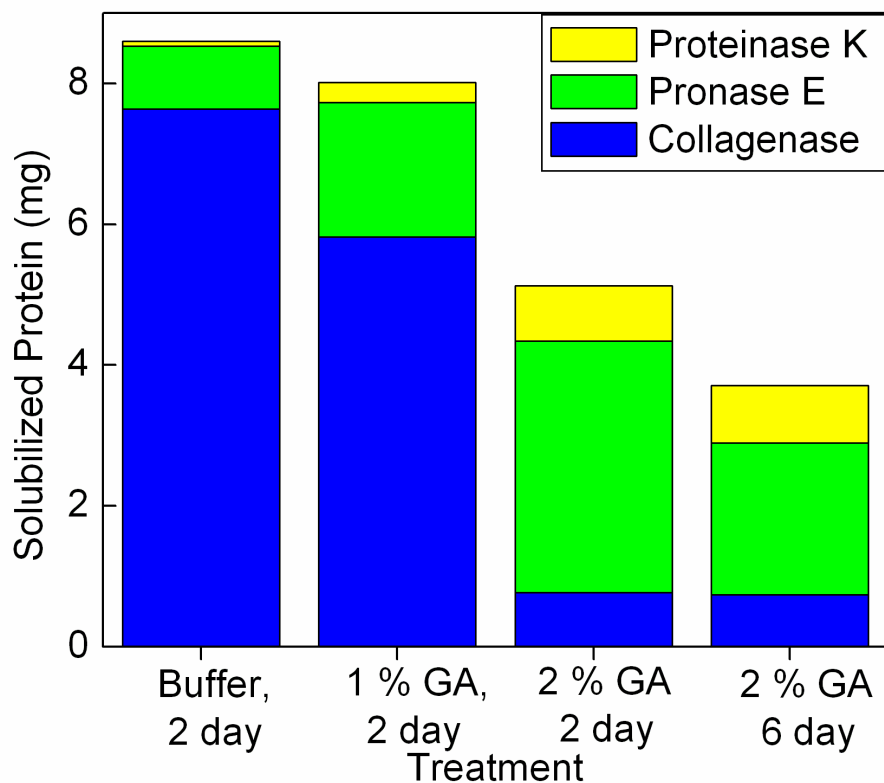


Figure 3. Glycated corneas resist enzymatic digestion. AGEs are likely to partition with the insoluble fraction; thus, concentrations of AGEs in enzymatic lysates do not necessarily represent concentrations in the intact tissue.

### 5.5 Quantification of Specific AGEs

As mentioned above, HPLC analysis of cornea lysates allowed us to isolate and quantify three known, acid-stable glyceraldehyde AGEs. Because enzymatic digestion proved ineffective for quantitative solubilization of cornea AGEs, acid hydrolysates were used. The total protein contents of all cornea hydrolysates were measured using the Ninhydrin method. Acid-labile AGEs are lost in this process, but arg-hydroxy-tiosidine, lys-hydroxy-triosidine, and argpyrimidine are quantitative markers of the extent of glycation: the level

of all three adducts increased upon treatment with GA (Figure 4). Neither arg-hydroxy-triosidine nor argpyrimidine were found in the acid hydrolysate solutions of the control corneas, and less than 400 pmol / mg total protein ( $358 \pm 273$  pmol / mg protein,  $n = 5$ ) of lys-hydroxy-triosidine were found. The 2-day rise in all three adducts was dose-dependent (lys-OH-triosidine: 1% GA –  $1427 \pm 89$ , 2% –  $2515 \pm 575$ ; arg-OH-triosidine: 1% GA –  $129 \pm 31$ , 2% –  $206 \pm 45$ ; argpyrimidine: 1% GA –  $2547 \pm 236$ , 2% –  $6011 \pm 1085$ ,  $n = 5$  in all cases) but, like rheological properties, adduct levels did not change significantly from day 2 to day 6 (for 2% GA – lys-OH-triosidine, day 6:  $2189 \pm 98$ ; arg-OH-triosidine, day 6:  $312 \pm 42$ ; argpyrimidine, day 6:  $5779 \pm 631$ ). Previous biochemical analyses in our labs have shown that additional AGEs will form with application of additional GA;<sup>14</sup> therefore, the lack of additional AGE formation from day 2 to day 6 indicates that all available GA reacts within two days— not that the cornea is saturated with AGEs.

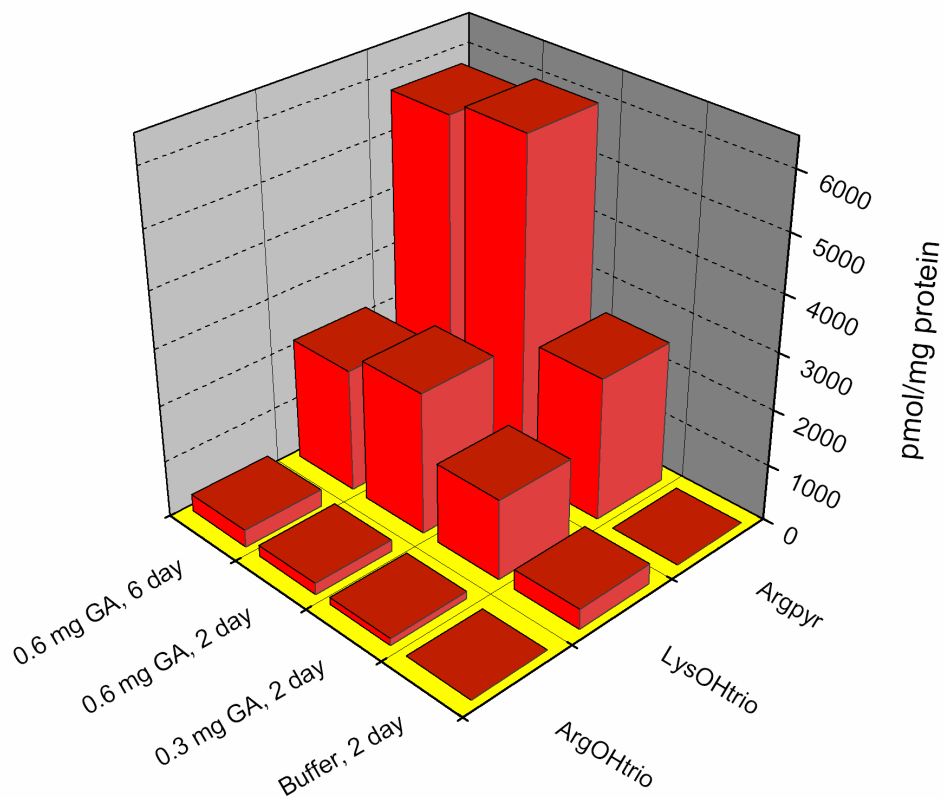


Figure 4. Three known glycerinaldehyde AGEs were found in treated corneas. Levels of all three adducts rose in a dose-dependent fashion, with argpyrimidine rising fastest, followed by lys-OH-triosidine and arg-OH-triosidine. Glycation appears to be complete after 2 days; additional incubation did not increase the levels of any of the three AGEs treated with 0.6 mg of GA.

Additionally, a strong linear relationship between AGE formation and shear modulus is apparent (Figure 5). Note that the intercept of the lys-OH-triosidine fit is different from the other two because it was the only AGE detected in control corneas. The diagnostic significance of this correlation will be explored in Section 5.7, where we will show that global tissue fluorescence can also be directly correlated with AGE formation and mechanical property changes.

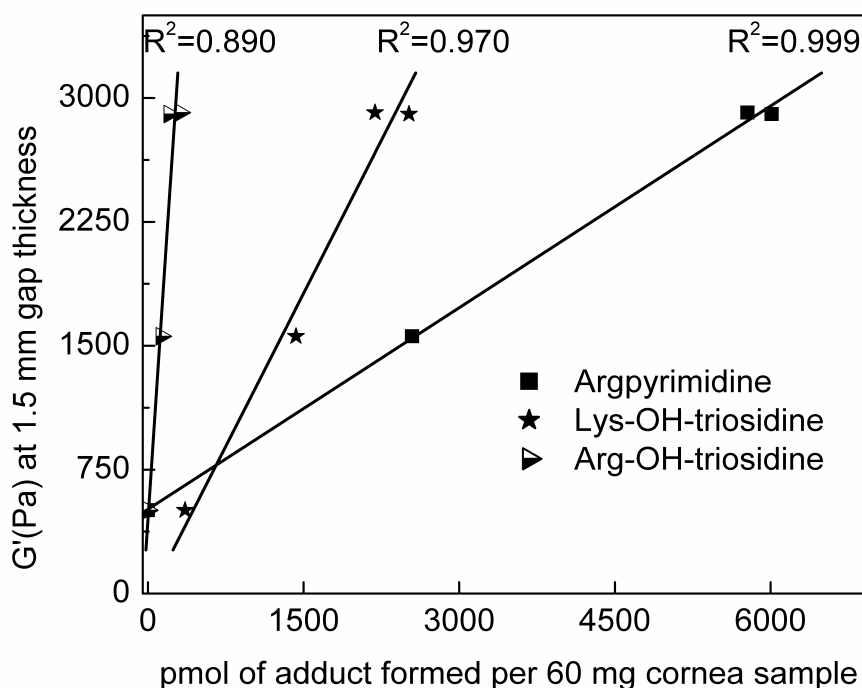


Figure 5. Shear modulus ( $G'$ ) of 60 mg cornea samples as a function of the quantity of three AGEs. After treatment and mechanical analysis, argpyrimidine, lys-hydroxy-triosidine, and arg-hydroxy-triosidine were quantified after 2 days in the control cornea, after 2 days using the 1% and 2% solutions, and after 6 days using the 2% solution. Modulus values and AGE content are nearly identical at 2 and 6 days, indicating that the tissue had been stabilized by glycation in two days or less. The  $R^2$  values for the best-fit lines of each adduct showed a high degree of linearity.

## 5.6 Solution and Solid-State NMR of Glycated Corneas

To investigate acid-labile AGEs in treated corneas, we have employed NMR analysis of tissue treated with isotopically labeled glyceraldehyde. Quantitative solid-state  $^{13}\text{C}$ -NMR was used to investigate *in situ* the nature of the major non-native resonances detectable in glycated corneal tissue and to compare with solution NMR difference spectra of enzymatically digested and acid hydrolyzed tissue; control spectra have been subtracted from all three (Figure 6). The signals from  $\sim 75 - 85$  ppm and from  $\sim 185 - 200$  ppm

disappeared upon acid hydrolysis, but have counterparts in the solution-state  $^{13}\text{C}$  NMR of the enzymatic lysate, suggesting they represent acid labile compounds.

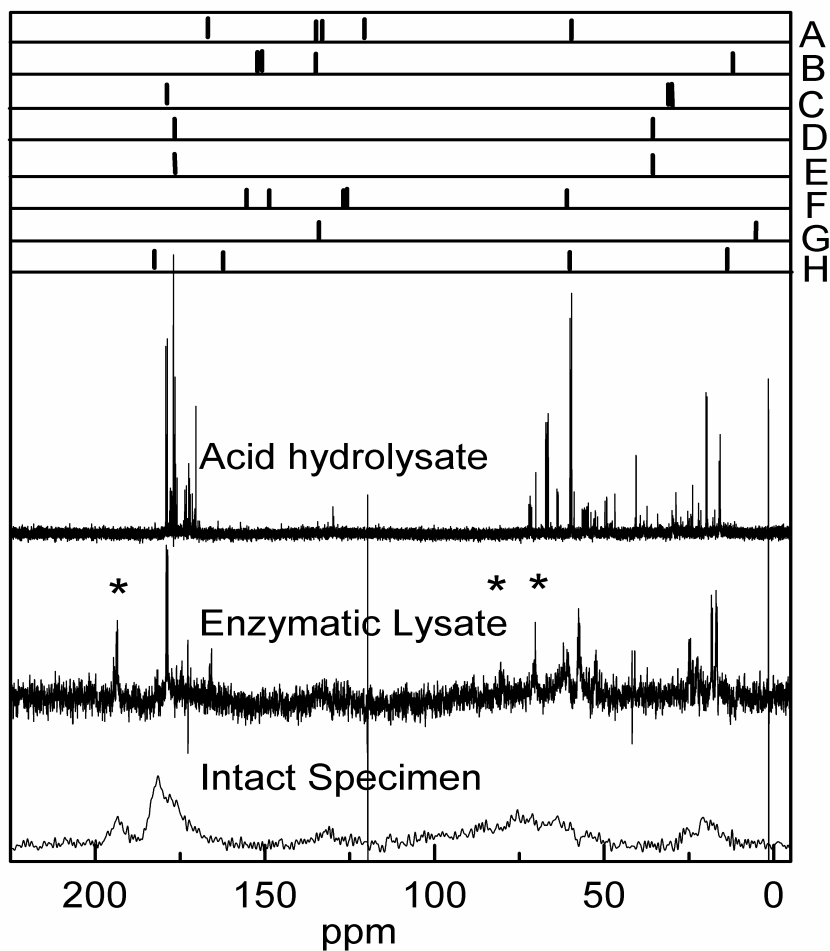


Figure 6. The solid-state 200 MHz  $^{13}\text{C}$  NMR spectrum of lyophilized, glycated porcine corneas ("intact specimen") compared with the 500 MHz solution NMR spectrum of equivalent corneas that have been dissolved by enzymatic digestion and by acid hydrolysis. Acetonitrile was used as a reference (120 ppm and 1.5 ppm). For reference, literature values of the chemical shifts of the known GA mediated AGEs are indicated above the spectra: A = arg-OH-triosidine, B = argpyrimidine, C = carboxy-ethyl-lysine (CEL), D = carboxy-methyl-arginine (CMA), E = carboxy-methyl-lysine (CML), F = lys-OH-triosidine, G = methylglyoxal-lysine dimer (MOLD), H = methylglyoxal-derived-imidazoline-cross-link (MODIC). Novel signals not attributable to known AGEs are indicated with asterisks (\*).

Resonances in Figure 6 are consistent with the published chemical shifts of CML, CEL, MOLD, CMA, and arg-OH-triosidine.<sup>3, 7, 8, 11, 14</sup> Resonances consistent with MODIC appear in solid-state and enzymatic-lysate spectra, but not in the acid hydrolysate.<sup>13</sup> Argpyrimidine and lys-OH-triosidine appear to be less significant.<sup>9, 14</sup> Because HPLC data showed that arg-OH-triosidine is present at lower concentrations than either argpyrimidine or lys-OH-triosidine (Figure 4), the lack of strong resonances from these two species suggests that resonances consistent with arg-OH-triosidine actually come from other species.

In addition to all expected AGEs, including acid labile adducts, the spectrum of the enzymatic lysate shows new, currently unexplained signals at 70, 81, and 193 – 195 ppm, as indicated by asterisks (Figure 6). These appear to be unsolved AGE structures that are inaccessible when using acid hydrolysis. As explained above, enzymatic lysates contain low concentrations of AGEs and additional losses due to precipitation were observed when lysate solutions were resuspended in D<sub>2</sub>O. Thus, the signal:noise ratio is too low to provide reliable data alone. However, similarities in the enzymatic lysate and solid-state spectra indicate that enzymatic digestion is a high-fidelity, albeit low yield method of sampling AGEs from tissue.

Finally, despite decades of AGE research, this experimental approach, combining NMR techniques and HPLC, is the first to gain a perspective on the fraction of all the glycation-induced modifications that are represented by specific AGEs in tissue specimens. Argpyrimidine illustrates the utility of this perspective. The symmetric ring carbons to which methyl groups are attached have a chemical shift of 150.3 ppm.<sup>9</sup> They originate in

GA and are  $^{13}\text{C}$  labeled; however, the 150.3 ppm peak is indistinguishable from the baseline in all three NMR spectra (Figure 6). Thus, the most abundant of the three adducts quantified in the present work contributes almost nothing to the observed NMR spectra. Comparing the chemical shifts of other known AGEs to the observed spectra reveals that known adducts can only account for a small fraction all AGEs. The AGE literature continues to expand rapidly and we hope that this accounting technique will be a useful tool for measuring our progress toward a more complete understanding of glycation. As we find ways to selectively inhibit or induce specific cross-links and examine the resulting tissue properties, solution and solid-state NMR used in tandem with rheology may also be invaluable for exploring the molecular basis of glycation-induced tissue stiffening.

### **5.7 Fluorescence – Noninvasive Indicator of Glycation**

The contribution of these three AGE fluorophores to the total fluorescence of the glycated corneas was found to account for at least 75% (90%, with 15% uncertainty) of the fluorescence at the global fluorescence emission maximum of the lysate solution (Figure 7). The global fluorescence excitation and emission maxima of enzymatically digested corneas treated with 2% GA for 2 days were 334 nm and 399 nm respectively. The “observed” spectrum shown is the difference spectrum of a treated cornea lysate minus the spectrum of a control cornea lysate (Figure 7). To estimate the fluorescence contribution due to the known AGEs, each of the three pure AGE solutions was excited at 334 nm and the emission spectrum was recorded, scaled to the mean concentration at which that adduct was found in the cornea, and added (“estimated” spectrum, Figure 7). Some discrepancy between the estimated and observed spectra is not surprising; we only account for the

contribution of three AGEs. Parallel experiments conducted using acid hydrolyzed corneas rather than enzymatically digested tissue yielded similar results (data not shown).

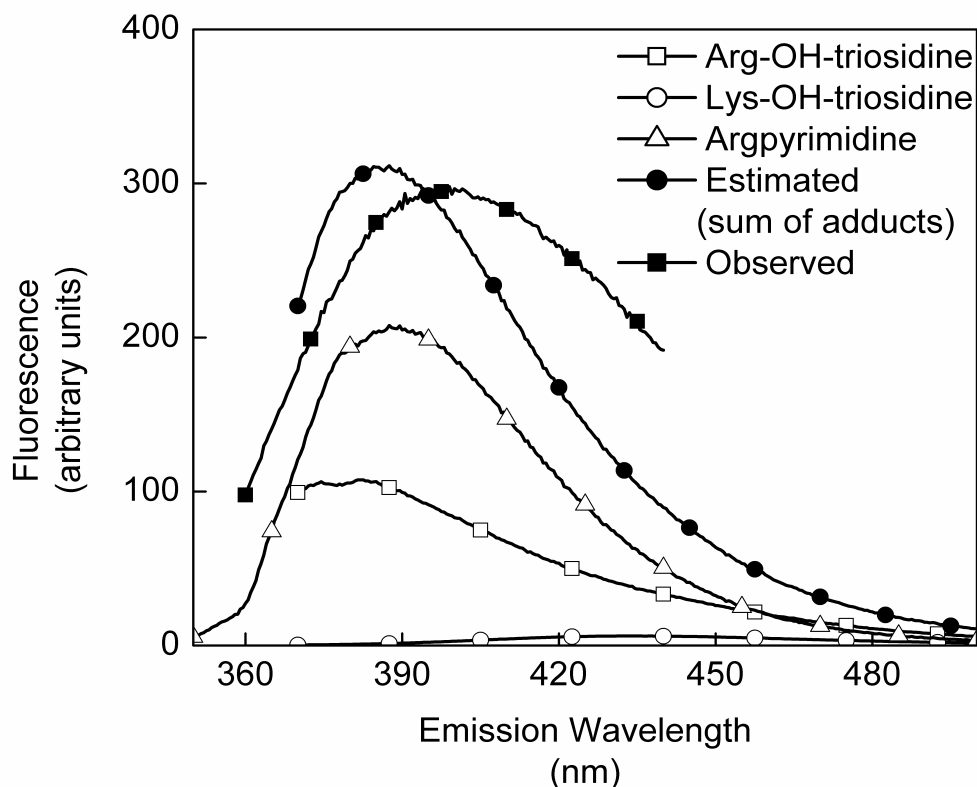


Figure 7. Fluorescence emission spectra ( $\lambda_{ex} = 334$  nm) of the cornea that was incubated for 6 days with 2% glyceraldehyde and solubilized by proteolytic digestion ("observed") and of pure solutions of arg-OH-triosidine, lys-OH-triosidine and argpyrimidine. The known adduct spectra are scaled to the mean concentration at which each adduct was found in the cornea. The estimated spectrum is the sum of these three spectra ("estimated").

It is significant that the rise of all three AGEs examined (including the non-cross-linking AGE argpyrimidine) correlate with stiffening, without regard to whether they are responsible for cross-linking. Because fluorescence can be quantitatively correlated with

the concentration of the fluorophores, the linear relation between fluorescent AGEs and shear modulus (Figure 5) also applies to fluorescence in the absence of quenching. Because linearity holds even in the highly-glycated cornea samples analyzed here, quenching is an unlikely problem for the much lower level of AGE accumulation expected in age and diabetes-related glycation. Indeed, fluorescence has recently been shown to be an accurate, noninvasive measure of AGE accumulation.<sup>44</sup> Thus, it should also be possible to indirectly measure the stiffness of collagenous tissues *in vivo* using an empirical relation between fluorescence and shear modulus.

The significant stiffening we have demonstrated with glyceraldehyde suggests that glycation is a promising engineering tool for soft collagenous tissues. We envision two areas of particular interest: bioadhesives and modulating the stiffness of implants. Glyceraldehyde crosslinks form between primary amines; therefore, if amines on adjacent tissues or a tissue and a synthetic implant are bound in the process, then they will be “glued” together. Collagen-based synthetic tissue replacements also have exposed lysine and arginine residues. Glycation may provide a relatively-biocompatible method for engineering the strength and modulus of synthetic biomaterials to match those of the target material.

Determining the chemical nature and location of the cross-links responsible for tissue stiffening and the reasons why they are correlated with the rise of the predominant AGEs will be an important area for future research. Our working hypothesis is that the kinetically favored cross-links are those that link amino acid side chains that are located in close proximity to each other within collagen fibrils. With the known sequence and alignment of

the three stands of the collagen I triple helix,<sup>45</sup> we have identified all 116 potential sites for the formation of crosslinks within collagen I triple helices based upon the number of Arg and Lys residues in proximity to each other. Due to the regularity of corneal collagen fibril diameter (30 nm)<sup>46</sup> and triple helix diameter (1.5 nm)<sup>31</sup>, we are also able to determine that there are ~ 400 helices / fibril and 46,545 potential crosslinking sites per 300 nm section of fibril (the approximate length of one triple helix). There are also 26 specific binding sites along corneal collagen fibrils per 300 nm section of fibril, where the protein cores of proteoglycans associate and could potentially be crosslinked, although the precise amino acids involved are not yet known.<sup>47</sup> If all potential crosslinking sites were occupied, there would be a maximum of 26 fibril-proteoglycan crosslinks vs. 46,545 intrafibrillar crosslinks per 300 nm fibril section (i.e., 1 fibril-proteoglycan crosslink per 2,327 intrafibrillar crosslinks). Since collagen fibrils represent 75% of the protein present in the stroma,<sup>36</sup> intrafibrillar AGEs are likely to dominate the NMR and fluorescence spectra. However, they may have little bearing on the mechanical modifications with which we are concerned.

Scott asserts that the mechanical properties of the bulk tissue are dominated by the fibril-proteoglycan interactions.<sup>48</sup> Thus, the adducts responsible for corneal stiffening may predominantly be those that covalently link proteoglycans to their binding sites. This implies that the mechanically-significant crosslinks are vastly outnumbered by *mechanically insignificant* intrafibrillar crosslinks. We will explore this hypothesis in greater depth in Chapter 6.

## BIBLIOGRAPHY

1. Hodge JE. Dehydrated foods, chemistry of browning reactions in model systems. *J. Agric. Food Chem.* 1953;1:928-943.
2. Sell DR, Monnier VM. Structure elucidation of a senescence cross-link from human extracellular matrix. Implication of pentoses in the aging process. *Journal of Biological Chemistry.* 1989;264:21597-21602.
3. Brinkmann E, Wells-Knecht KJ, Thorpe SR, Baynes JW. Characterization of an imidazolium compound formed by reaction of methylglyoxal and N-alpha-hippuryllysine. *J. Chem. Soc. Perkin. T.1.* 1995;22:2817-2818.
4. Wells-Knecht KJ, Brinkmann E, Baynes JW. Characterization of an imidazolium salt formed from glyoxal and N-alpha-hippuryllysine – A model for Maillard reaction cross-links in proteins. *J. Org. Chem.* 1995;60(1995):6246-6247.
5. Tessier F, Obrenovich M, Monnier VM. Structure and mechanism of formation of human lens fluorophore LM-1 – Relationship to vesperlysine A and the advanced Maillard reaction in aging, diabetes, and cataractogenesis. *Journal of Biological Chemistry.* 1999;274:20796-20804.
6. Nagaraj RH, Portero-Otin M, Monnier VM. Pyrroline ether crosslinks as a basis for protein crosslinking by the advanced Maillard reaction in aging and diabetes. *Arch. Biochem. Biophys.* 1996;325:152-158.
7. Ahmed MU, Thorpe SR, Baynes JW. Identification of N epsilon-carboxymethyllysine as a degradation product of fructoselysine in glycated protein. *Journal of Biological Chemistry.* 1986;261:4889-4894.
8. Ahmed MU, Frye EB, Degenhardt TP, Thorpe SR, Baynes JW. N-epsilon-(carboxyethyl)lysine, a product of the chemical modification of proteins by methylglyoxal, increases with age in human lens proteins. *Biochem. J.* 1997;324:565-570.
9. Shipanova IN, Glomb MA, Nagaraj RH. Protein modification by methylglyoxal: chemical nature and synthetic mechanism of a major fluorescent adduct. *Arch. Biochem. Biophys.* 1997;344:29-36.
10. Lo TW, Westwood ME, McLellan AC, Selwood T, Thornalley PJ. Binding and modification of proteins by methylglyoxal under physiological conditions. A kinetic and mechanistic study with N alpha-acetylarginine, N alpha-acetylcysteine, and N alpha-acetyllysine, and bovine serum albumin. *J Biol Chem.* Dec 23 1994;269(51):32299-32305.
11. Iijima K, Murata M, Takahara H, Irie S, Fujimoto D. Identification of N(omega)-carboxymethylarginine as a novel acid-labile advanced glycation end product in collagen. *Biochem J.* Apr 1 2000;347 Pt 1:23-27.
12. Glomb MA, Pfahler C. Amides are novel protein modifications formed by physiological sugars. *Journal of Biological Chemistry.* Nov 9 2001;276(45):41638-41647.
13. Lederer MO, Klaiber RG. Cross-linking of proteins by maillard processes: characterization and detection of lysine-arginine cross-links derived from

- glyoxal and methylglyoxal. *Bioorganic & Medicinal Chemistry*. 1999/11 1999;7(11):2499-2507.
14. Tessier FJ, Monnier VM, Sayre LA, Kornfield JA. Triosidines: Novel maillard reaction products and crosslinks from the reaction of triose sugars with lysine and arginine residues. *Biochem J*. Oct 14 2002;Pt.
  15. Andreassen TT, Oxlund H. Thermal stability of collagen in relation to non-enzymatic glycosylation and browning in vitro. *Diabetologia*. Sep 1985;28(9):687-691.
  16. Reiser KM. Nonenzymatic glycation of collagen in aging and diabetes. *Proc Soc Exp Biol Med*. Jan 1991;196(1):17-29.
  17. Bruel A, Oxlund H. Changes in biomechanical properties, composition of collagen and elastin, and advanced glycation endproducts of the rat aorta in relation to age. *Atherosclerosis*. Dec 20 1996;127(2):155-165.
  18. Sims TJ, Rasmussen LM, Oxlund H, Bailey AJ. The role of glycation cross-links in diabetic vascular stiffening. *Diabetologia*. Aug 1996;39(8):946-951.
  19. Sady C, Khosrof S, Nagaraj R. Advanced Maillard reaction and crosslinking of corneal collagen in diabetes. *Biochem Biophys Res Commun*. Sep 25 1995;214(3):793-797.
  20. Baynes JW, Monnier VM. *The Maillard Reaction in Ageing, Diabetes and Nutrition*. New York: A. R. Liss; 1989.
  21. McCance DR, Dyer DG, Dunn JA, et al. Maillard reaction products and their relation to complications in insulin-dependent diabetes mellitus. *J Clin Invest*. Jun 1993;91(6):2470-2478.
  22. Vitek MP, Bhattacharya K, Glendening JM, et al. Advanced glycation end products contribute to amyloidosis in Alzheimer disease. *Proc Natl Acad Sci U S A*. May 24 1994;91(11):4766-4770.
  23. Airaksinen KE, Salmela PI, Linnaluoto MK, Ikaheimo MJ, Ahola K, Ryhanen LJ. Diminished arterial elasticity in diabetes: association with fluorescent advanced glycosylation end products in collagen. *Cardiovasc Res*. Jun 1993;27(6):942-945.
  24. Vogel HG. Influence of maturation and age on mechanical and biochemical parameters of connective tissue of various organs in the rat. *Connect Tissue Res*. 1978;6(3):161-166.
  25. Galeski A, Kastelic J, Baer E, Kohn RR. Mechanical and structural changes in rat tail tendon induced by alloxan diabetes and aging. *J Biomech*. 1977;10(11/12):775-782.
  26. Duquette JJ, Grigg P, Hoffman AH. The effect of diabetes on the viscoelastic properties of rat knee ligaments. *J Biomech Eng*. Nov 1996;118(4):557-564.
  27. Girton TS, Oegema TR, Tranquillo RT. Exploiting glycation to stiffen and strengthen tissue equivalents for tissue engineering. *J Biomed Mater Res*. Jul 1999;46(1):87-92.
  28. Tae G, et al. In preparation.
  29. Spoerl E, Seiler T. Techniques for stiffening the cornea. *J Refract Surg*. Nov-Dec 1999;15(6):711-713.

30. Stryer I. Glycation of albumin: reaction with glucose, fructose, galactose, ribose or glyceraldehyde measured using four methods. *J Biochem Biophys Methods*. Mar 1994;28(2):115-121.
31. Stryer L. *Biochemistry*. 4th ed. New York: W. H. Freeman and Co.; 2000.
32. Wollensak G, Spoerl E, Seiler T. Treatment of keratoconus by collagen cross linking. *Ophthalmologe*. Jan 2003;100(1):44-49.
33. Wollensak G, Spoerl E, Seiler T. Stress-strain measurements of human and porcine corneas after riboflavin-ultraviolet-A-induced cross-linking. *Journal Of Cataract And Refractive Surgery*. Sep 2003;29(9):1780-1785.
34. Wollensak G, Spoerl E, Wilsch M, Seiler T. Keratocyte apoptosis after corneal collagen cross-linking using riboflavin/UVA treatment. *Cornea*. Jan 2004;23(1):43-49.
35. Fatt I, Weissman BA. *Physiology of the Eye*. Second ed. Boston: Butterworth-Heinemann; 1992.
36. Davson H. *The Eye*. Vol 1. fifth ed. New York: Academic Press; 1990.
37. Rehany U, Lahav M, Shoshan S. Collagenolytic activity in keratoconus. *Ann Ophthalmol*. 1982 Aug 1982;14(8):751-754.
38. Abalain JH, Dossou H, Colin J, Floch HH. Levels of collagen degradation products (telopeptides) in the tear film of patients with keratoconus. *Cornea*. Jul 2000;19(4):474-476.
39. Kao WWY, Vergnes JP, Ebert J, Sundarraj CV, Brown SI. Increased Collagenase And Gelatinase Activities In Keratoconus. *Biochemical And Biophysical Research Communications*. 1982;107(3):929-936.
40. Smith VA, Easty DL. Matrix metalloproteinase 2: involvement in keratoconus. *European Journal Of Ophthalmology*. Jul-Sep 2000;10(3):215-226.
41. Lema I, Duran JA. Inflammatory molecules in the tears of patients with keratoconus. *Ophthalmology*. Apr 2005;112(4):654-659.
42. Fukuchi T, Yue B, Sugar J, Lam S. Lysosomal-Enzyme Activities In Conjunctival Tissues Of Patients With Keratoconus. *Archives Of Ophthalmology*. Oct 1994;112(10):1368-1374.
43. Kochakian M, Manjula BN, Egan JJ. Chronic dosing with aminoguanidine and novel advanced glycosylation end product-formation inhibitors ameliorates cross-linking of tail tendon collagen in STZ-induced diabetic rats. *Diabetes*. Dec 1996;45(12):1694-1700.
44. Meerwaldt R, Graaff R, Oomen PHN, et al. Simple non-invasive assessment of advanced glycation endproduct accumulation. *Diabetologia*. Jul 2004;47(7):1324-1330.
45. Meek KM, Chapman JA, Hardcastle RA. Staining Pattern Of Collagen Fibrils - Improved Correlation With Sequence Data. *Journal Of Biological Chemistry*. 1979;254(21):710-714.
46. Oyster CW. *The Human Eye: Structure and Function*. Sunderland, MA: Sinauer Associates, Inc.; 1999.
47. Yu L, Cummings C, Sheehan JK, Kadler K, Holmes DF, Chapman JA. *Dermatan Sulphate Proteoglycans: Chemistry, Biology, Chemical Pathology*. Chapel Hill: Portland Press Inc.; 1993.

48. Scott JE. Extracellular matrix, supramolecular organisation and shape. *J Anat.* Oct 1995;187 (Pt 2):259-269.